Supplemental Table 1. Number of DOTA per αCD11b antibody on DOTA-αCD11b conjugate

DOTA/ αCD11b ratio	50:1
Number of DOTA per αCD11b	5.77 ± 0.394

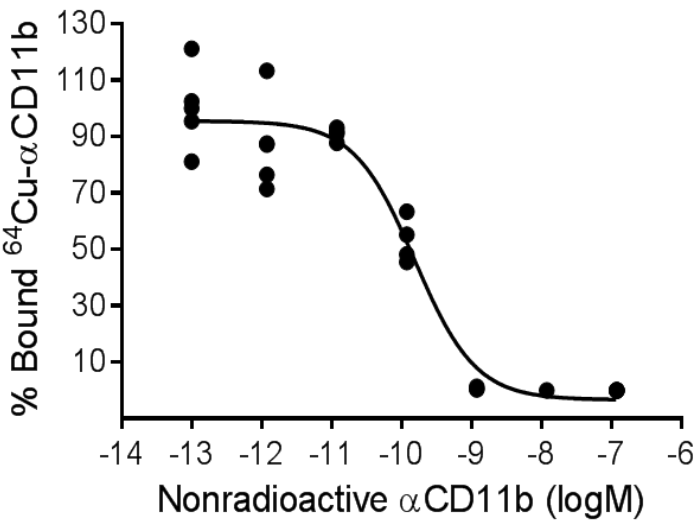

Supplemental Figure 1. Cell binding assay. Displacement of the binding of ^{64}Cu-αCD11b to bone marrow cells by nonradioactive αCD11b (n=5).

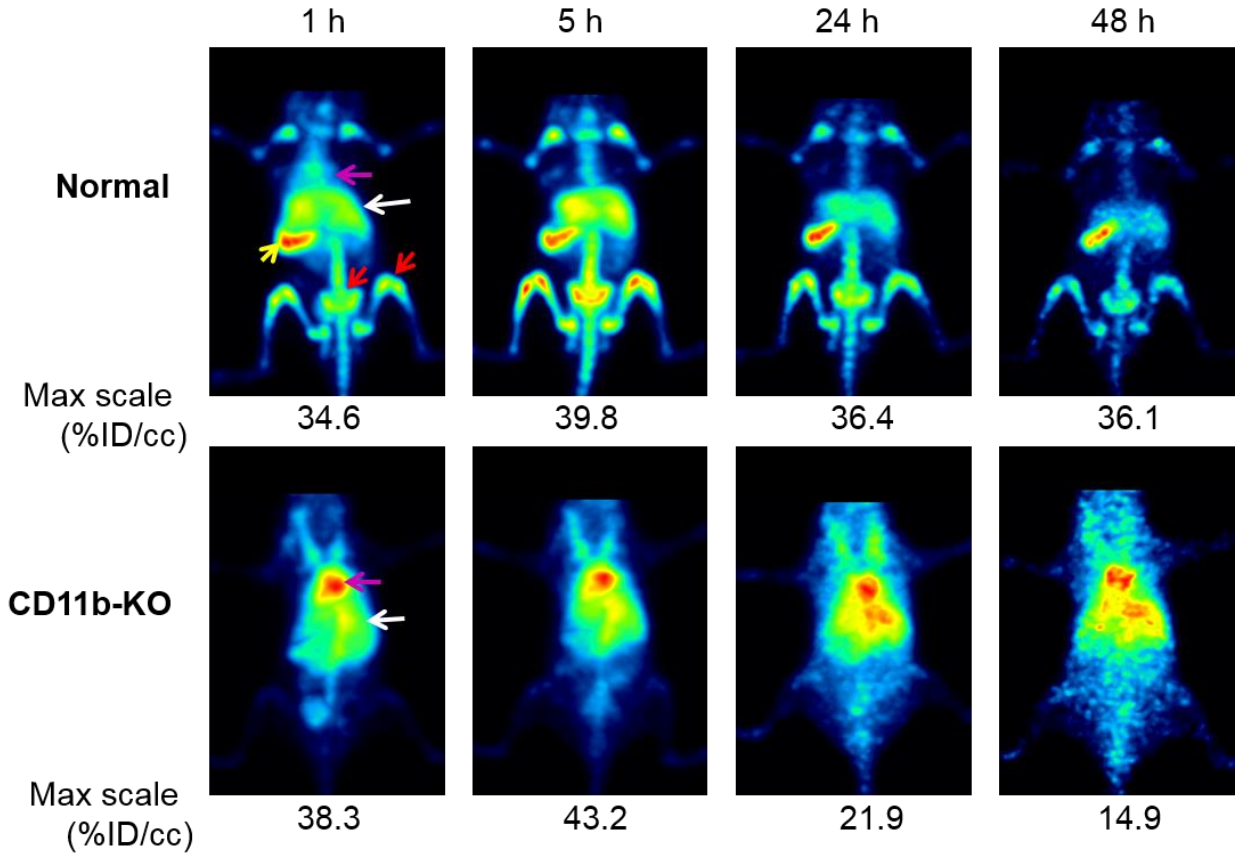

Supplemental Figure 2. Representative 3D maximum intensity projection (MIP) µPET images with ^{64}Cu-αCD11b on normal and CD11b knockout (CD11b-KO) C57BL/6 mice.

Red arrows: bone marrow; yellow arrows: spleen; white arrows: liver; purple arrows: heart (n=3).

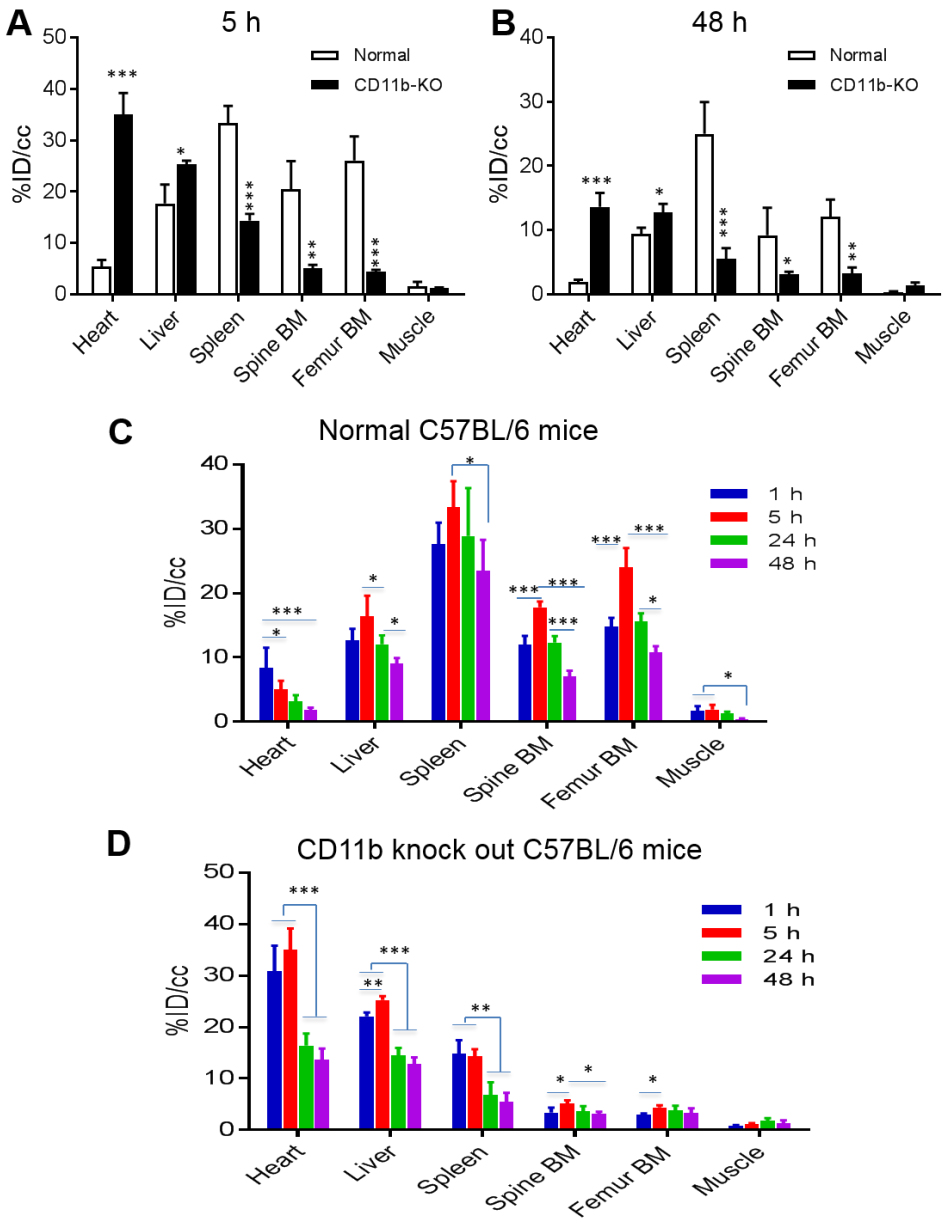

Supplemental Figure 3. Quantitative analysis of µPET/CT imaging data of ^{64}Cu-αCD11b in normal and CD11b-KO C57BL/6 mice. (**A, B**) Quantity analysis µPET/CT imaging data acquired at 5 h (**A**) or 48 h (**B**) after intravenous injection of ^{64}Cu-αCD11b. (**C, D**) Quantity µPET/CT imaging data in normal C57BL/6 mice (**C**) and CD11b-KO C57BL/6 mice (**D**) at 1, 5, 24, and 48 h after radiotracer injection. Data are expressed as mean ± SD (n=3/group).

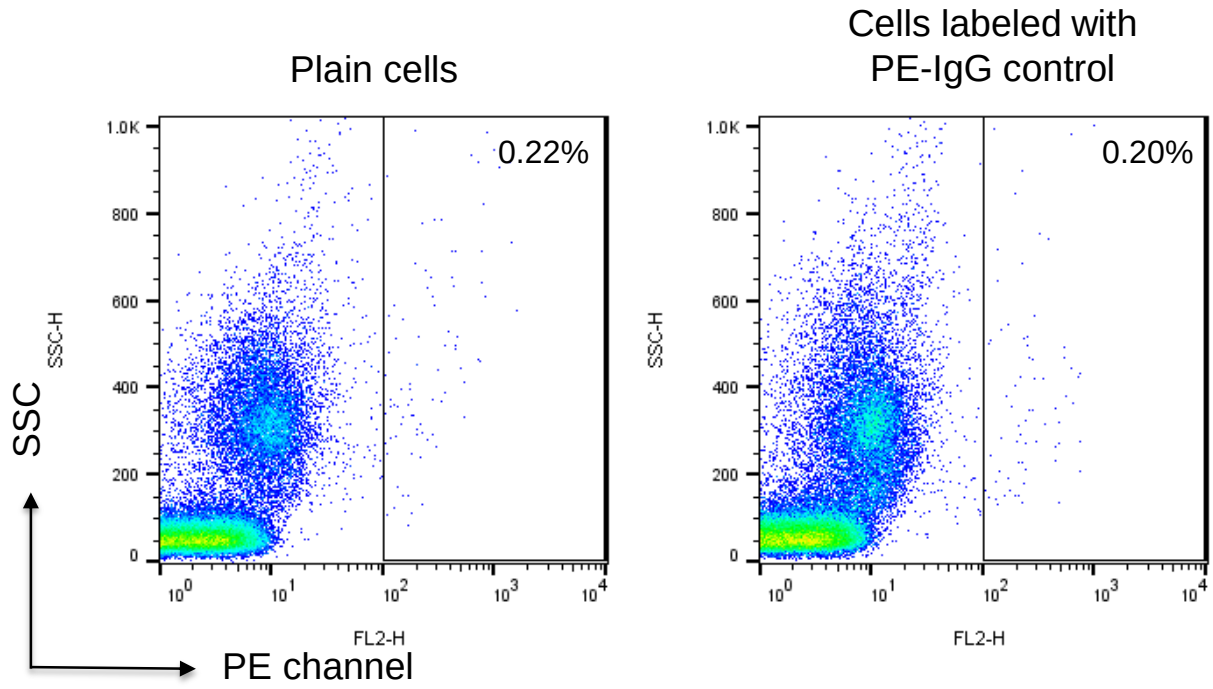

Supplemental Figure 4. Dot plot diagram of flow cytometry showing background signals from the PE channel for plain bone marrow cells and bone marrow cells treated with PE-IgG control.

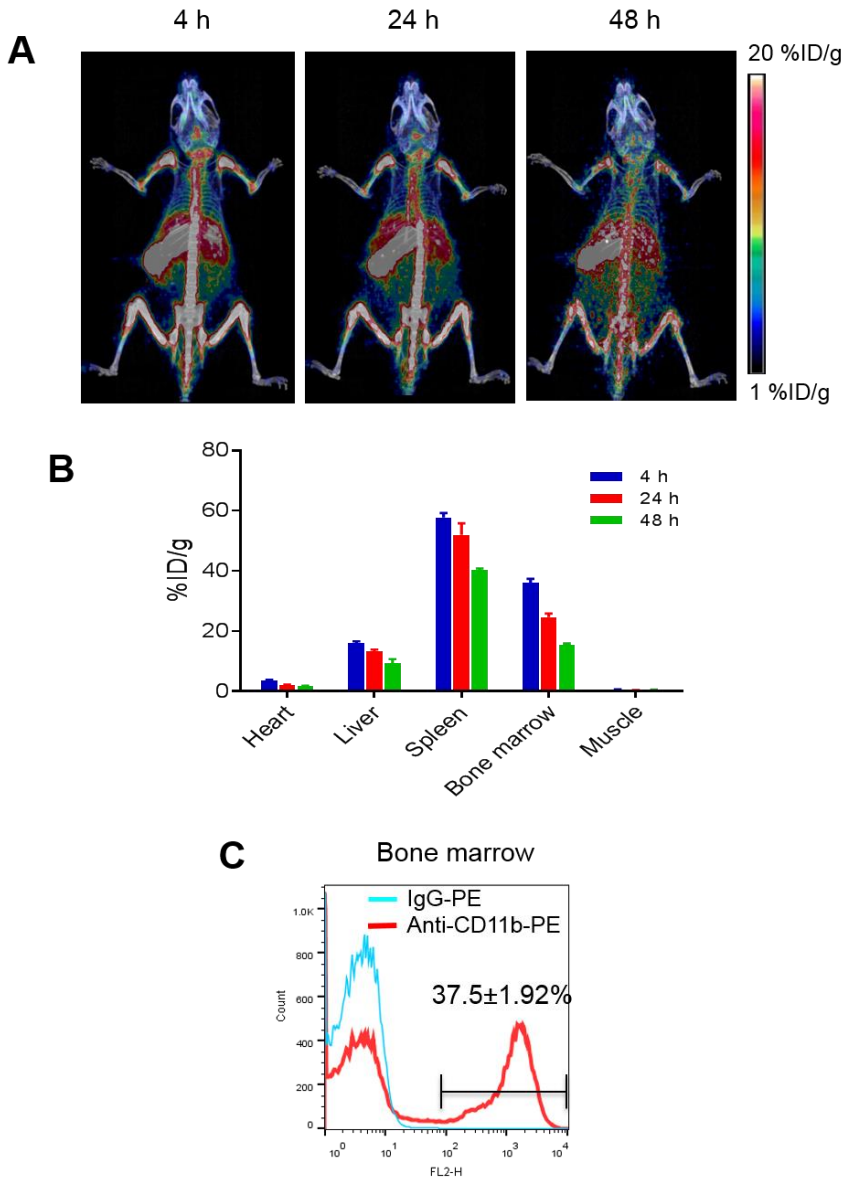

Supplemental Figure 5. ^{64}Cu-αCD11b μPET/CT in normal BALB/c mice. (**A**) Representative μPET/CT images of normal BALB/c mice at 4, 24, and 48 h after intravenous injection of ^{64}Cu-αCD11b. (**B**) Quantitative analysis of μPET/CT data showing distribution of ^{64}Cu-αCD11b in major organs at different times after radiotracer injection. (**C**) Flow cytometry analysis of CD11b^{+} myeloid cells in bone marrow. The resting bone marrow contains a large number of CD11b^{+} myeloid cells in BALB /c mice. Data were expressed as mean ± SD (n=3).

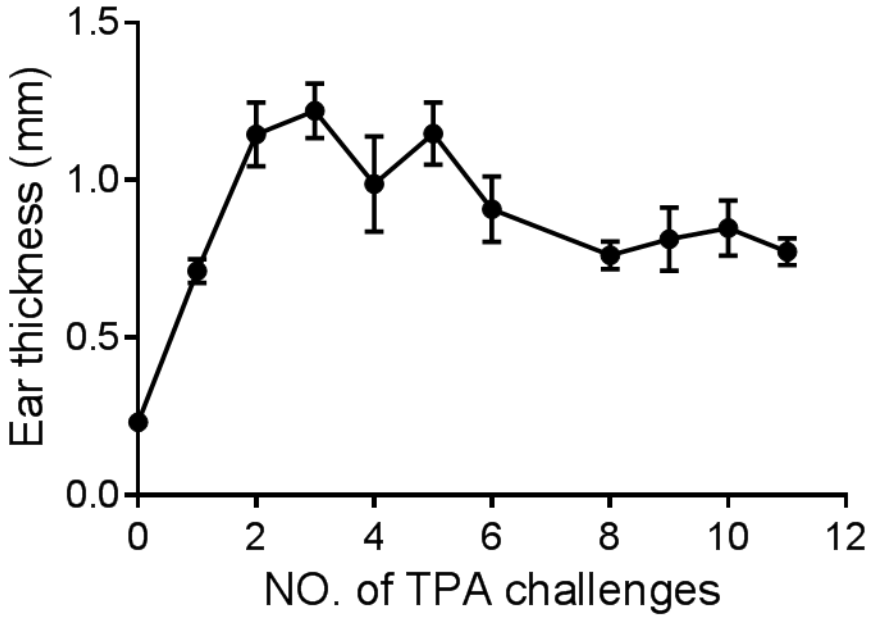

Supplemental Figure 6. Ear thickness after different numbers of TPA challenges on ear of BALB/c mice. Data are expressed as mean ± SD (n=8).

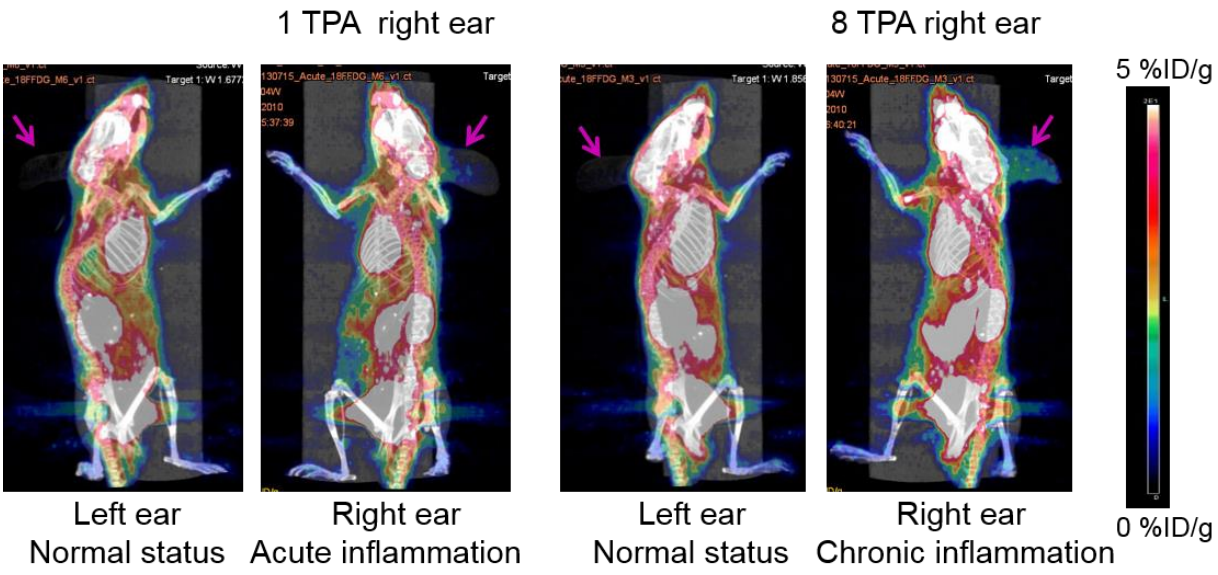

Supplemental Figure 7. 18F-FDG µPET/CT in BALB/c mice with TPA-induced acute and chronic ear inflammation. Images were presented at a color scale (0 – 5 %ID/g) different from that in Figure 3C (3 – 10 %ID/g) to highlight uptake of the radiotracer in the inflammation ear. Purple arrow: ear.

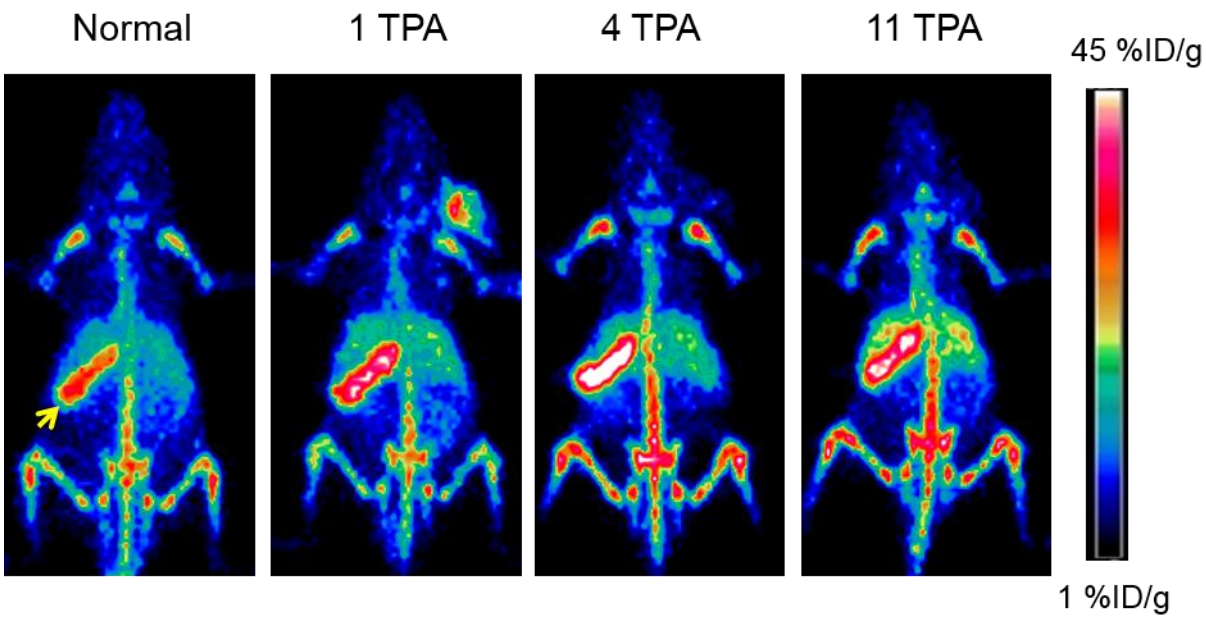

Supplemental Figure 8. ^{64}Cu-αCD11b μPET/CT in BALB/c mice with TPA-induced acute and chronic ear inflammation. Images were presented at a color scale (1 – 45 %ID/g) different from that in Figure 2 (1 – 20 %ID/g) to highlight changes in the spleen after different numbers of TPA challenges. Yellow arrow: spleen.

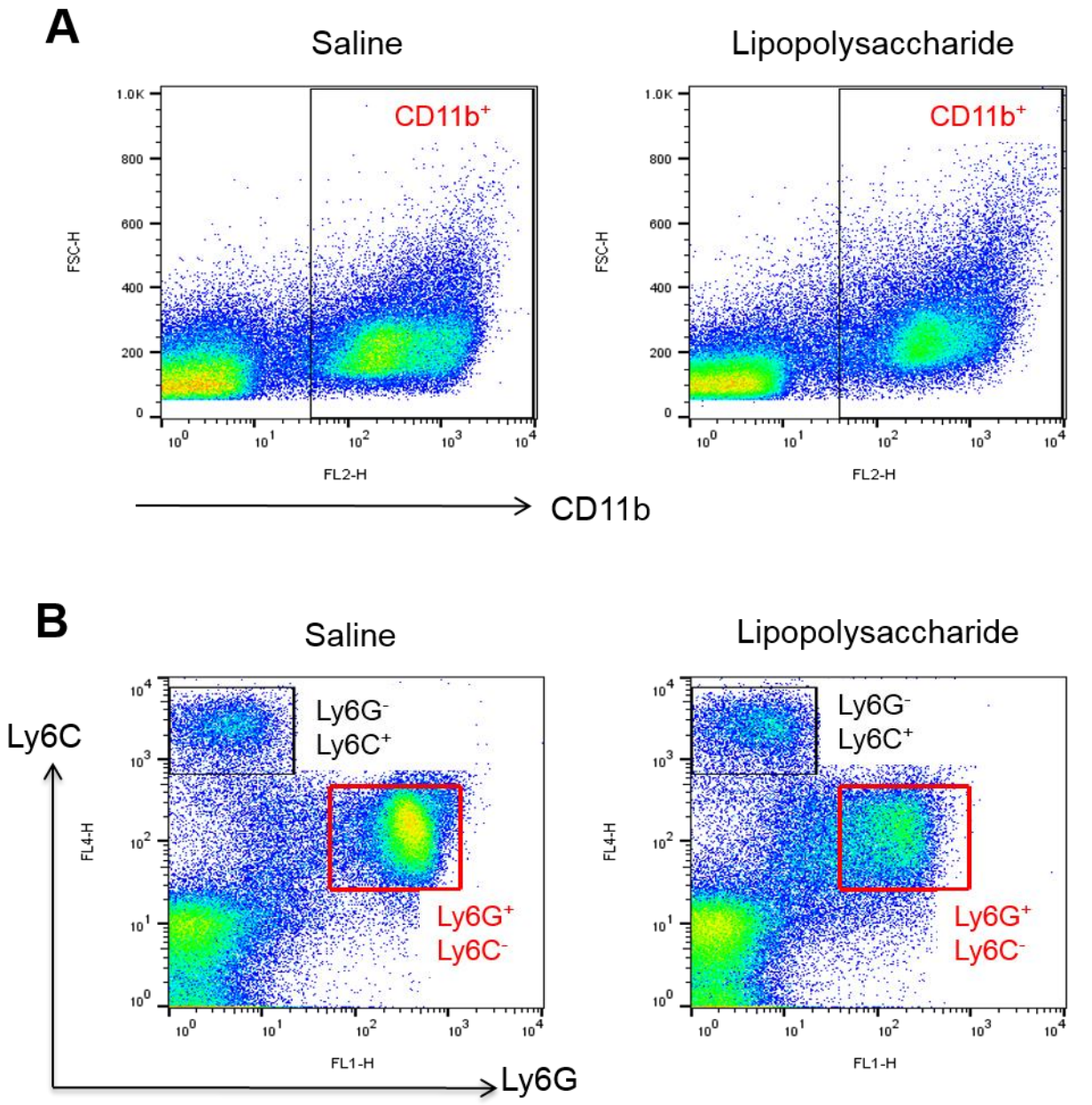

Supplemental Figure 9. The representative flow cytometric dot plots showing bone marrow cells from normal mice and mice with acute lung inflammation. Bone marrow cell samples were analyzed 24 h after intratracheal instillation of lipopolysaccharide. (**A**) Black grid: $CD11b^+$ cells. (**B**) Black grid: $Ly6G^-Ly6C^+$ monocytic cells; red grid: $Ly6G^+Ly6C^{low}$ granulocytic cells.